Phosphorylation States of Microtubule-Associated Protein 2 (MAP2) Determine the Regulatory Role of MAP2 in Microtubule Dynamics†

Tomohiko J. Itoh,*,‡ Shin-ichi Hisanaga,§,|| Tomoko Hosoi,§ Takeo Kishimoto,§ and Hirokazu Hotani‡

Division of Biological Science, Graduate School of Science, Nagoya University, Furo-cho, Chikusa-ku, Nagoya 464-01, Japan, and Laboratory of Cell and Developmental Biology, Faculty of Biosciences, Tokyo Institute of Technology, Nagatsuta, Midori-ku, Yokohama 226, Japan

Received October 17, 1996; Revised Manuscript Received July 30, 1997⊗

ABSTRACT: Phosphorylation-dependent regulation of microtubule-stabilizing activities of microtubule-associated protein 2 (MAP2) was examined using optical microscopy. MAP2, purified from mammalian brain, was phosphorylated by either cAMP-dependent protein kinase (PKA) or cyclin B-dependent cdc2 kinase. Using PKA, 15 mol of phosphoryl groups was incorporated per mole of MAP2, but about 70% of the phosphates was distributed to the projection region. Using cdc2 kinase, 7−10 mol of phosphoryl groups was incorporated per mole of MAP2, and more than 60% of the phosphates was distributed to the microtubule-binding region. Both types of phosphorylation similarly reduced binding activity of MAP2 onto microtubules. Direct observation of individual microtubules using dark-field microscopy showed that interconversion between the polymerization phase and the depolymerization phase was repeated in both unphosphorylated and PKA-phosphorylated MAP2. In cdc2 kinase-phosphorylated MAP2, however, the phase transition from depolymerization to polymerization occurred with difficulty, with the result being that the half-life of individual microtubules was as short as in the absence of MAP2. Examination of spontaneous polymerization of microtubules using dark-field microscopy showed that the microtubule-nucleating activity of MAP2 was reduced by PKA-dependent phosphorylation and was completely abolished by cdc2 kinase-dependent phosphorylation. These observations show that cdc2 kinase-dependent phosphorylation inhibits both the microtubule-stabilizing activity and the microtubule-nucleating activity of MAP2, while PKA-dependent phosphorylation affects only the microtubule-nucleating activity of MAP2.

Microtubules are cylindrical polymers of α and β tubulin heterodimers, and a variety of minor components called microtubule-associated proteins (MAPs)[1] are bound to their outer surfaces. Microtubules are common to most eukaryotic cells and are involved in many cellular processes, for example, chromosome segregation and determination of cell polarity (for review, see refs 1 and 2). One of the most prominent features of cytoplasmic microtubules is their dynamic behavior, that is, their rapid polymerization and depolymerization *in vivo*.

Individual microtubules repeat alternating phases of polymerization and depolymerization both *in vitro* and in living cells, a process known as "dynamic instability" (*3*−*7*). In cell free systems, MAPs have been shown to regulate the dynamic instability especially by increasing the frequency of rescue (*8*−*12*). This regulation of microtubule dynamics has also been suggested to depend on the cooperative binding of MAPs to the microtubule surface (*11*), and thus, one can experimentally modulate the dynamic behavior of individual microtubules by changing the concentration of MAPs. It might be expected that binding of MAPs to microtubules also regulates microtubule dynamics in living cells, but within living cells, the direct increase or decrease of the amount of MAPs would appear to be improbable. Rather, other mechanisms controlling their binding activity and/or their ability to regulate microtubule dynamics are probably necessary.

Among various MAPs, heat-stable MAPs, including microtubule-associated protein 2 (MAP2), microtubule-associated protein 4 (MAP4), and tau, have been well characterized, and they possess a common structural property; i.e., they are long fibrous molecules made up of a C-terminal microtubule-binding domain and a long N-terminal projection domain which extends freely from the microtubule surface (*13*). These heat-stable MAPs possess the ability to stabilize microtubules especially by increasing the frequency of rescue (for example, see ref 11).

Recently, we demonstrated that MAP4, a major MAP in HeLa cells, (1) was associated with the cdc2 kinase/cyclin B complex in living cells, (2) was phosphorylated by the kinase; and (3) abolished its microtubule-stabilizing activity following phosphorylation but without decreasing its binding activity (*14*). Individual microtubules were quite labile in the presence of phosphorylated MAP4 due to the decreased rescue frequency, while MAP4 in an unphosphorylated state readily stopped microtubule depolymerization. The sum of these data constitutes strong evidence which shows that cell

† This work was supported by Grants-in-Aids for Scientific Research from the Ministry of Education, Science and Culture of Japan (to T.J.I., S.H., H.H., and T.K.).

‡ Nagoya University.

§ Tokyo Institute of Technology.

|| Present address: Department of Biology, Faculty of Science, Tokyo Metropolitan University, Minamiosawa 1-1, Hachioji-shi, Tokyo 192-03, Japan.

⊗ Abstract published in *Advance ACS Abstracts,* September 15, 1997.

[1] Abbreviations: EGTA, ethylene glycol bis(β-aminoethyl ether)-*N*,*N*,*N*′,*N*′-tetraacetic acid; GTP, guanosine 5′-triphosphate; MAP, microtubule-associated protein; MOPS, 3-morpholinopropanesulfonic acid; PIPES, piperazine-1,4-bis(2-ethanesulfonic acid); PKA, type II cAMP-dependent protein kinase; PM buffer, 0.1 M PIPES (pH 6.9), 0.5 mM $MgSO_4$, and 1 mM EGTA; SDS−PAGE, sodium dodecyl sulfate−polyacrylamide gel electrophoresis.

S0006-2960(96)02606-2 CCC: $14.00

cycle-dependent changes in microtubule dynamics are directly regulated by cdc2 kinase/cyclin B-dependent phosphorylation, a cell cycle controlling factor (*15*).

A major MAP of the *Xenopus* egg, termed p220, was also shown to be phosphorylated especially during the M phase, by cdc2 kinase/cyclin B and MAP kinase. p220 isolated from interphase egg extracts stimulates microtubule polymerization, while the phosphorylated p220 does not (*16*). These findings indicate that phosphorylation is an important parameter that physiologically modulates the activity of MAPs which in turn regulates microtubule dynamics during the cell cycle.

In the central nervous system, where microtubules are especially abundant, they play an essential role in the organization and function of axonal and dendritic processes of neurons. Major MAPs in mammalian brain include microtubule-associated protein 1 (MAP1), MAP2, and tau, which have already been extensively investigated (*2*, *17*). Among them, MAP2 is multiply phosphorylated, especially in living tissue, in which up to 46 phosphoryl groups can be incorporated per mole of MAP2 (*18*). Indeed, MAP2 is a good substrate of various kinases *in vitro*, such as type II cAMP-dependent protein kinase (PKA) (*19*, *20*), Ca^{2+}/calmodulin-dependent protein kinase (*21*, *22*), protein kinase C (*23*, *24*), MAP kinase (*25*), cyclin B-dependent cdc2 kinase (*26*), protein kinase $p110^{mark}$ (*27*), and an unidentified brain endogenous kinase (*28*). The multiple phosphorylations by various kinases, including second messenger-dependent ones, evoke the idea that MAP2 could be critical to the signaling of processing during neuron activity. The phosphorylation of MAP2 may also play a part in neuronal plasticity (*13*).

Little is known about which kinase is actually involved in the physiological regulation of microtubules *in vivo*. Effects of phosphorylation of MAP2 by various kinases have been primarily studied using turbidimetry, the result being that they similarly inhibited MAP2 activity which stimulates microtubule polymerization. However, the effects of phosphorylation of MAP2 on the dynamics of individual microtubules have not yet been established. Analyzing the effect of MAP2 phosphorylation on microtubule dynamics should provide a molecular basis for the regulation of this cytoskeletal component. Among known kinases, PKA and cdk5 kinases copurify with brain microtubule protein and are associated with microtubules (*29*−*32*). Brain cdk5 is a cdc2-related kinase, which phosphorylates Ser or Thr residues following a proline residue; namely, it is a proline-directed kinase (*32*). This cdk5 kinase was recently shown to be a major phosphorylating kinase for tau, another heat-stable MAP abundant in the axons (*33*). The association of kinases with microtubules gives rise to the idea that both kinases catalyze the phosphorylation of MAP2 *in vivo* and might participate in the regulation of cytoskeletal organization.

In this study, we examined the influence of MAP2 phosphorylation on microtubule dynamics. We compared MAP2 phosphorylated by PKA with that phosphorylated by cyclin B-dependent cdc2 kinase. To investigate the proline-directed phosphorylation, we used cyclin B-dependent cdc2 kinase instead of cdk5 since both kinases have similar substrate specificities and phosphorylate the same sites in tau (*32*, *34*). We demonstrate in this study that, independent of the basal level of phosphorylation, MAP2 incorporates about 15 phosphoryl groups by the former kinase and 7−10 by the latter. PKA primarily phosphorylates the projection region of MAP2, while cyclin B-dependent cdc2 kinase phosphorylated primarily the microtubule-binding region. Both phosphorylations similarly decreased the binding activity of MAP2 to microtubules. However, phosphorylation by PKA does not reduce one activity of MAP2, that of increasing the frequency of rescue, while it suppresses another activity of MAP2, that of stimulating the self-nucleation of microtubules. In contrast, phosphorylation of MAP2 by cyclin B-dependent cdc2 kinase clearly decreases both activities of MAP2. We suggest therefore that different phosphorylation states, which depend on these two distinct kinases, differently determine the MAP2 functional activities which regulate microtubule dynamics.

EXPERIMENTAL PROCEDURES

Protein Preparations. Tubulin and MAP2 were purified from microtubule proteins of bovine or porcine brain by the method described previously (*35*). Microtubule proteins were prepared by three cycles of temperature-dependent polymerization and depolymerization as described by Karr et al. (*36*), and from this preparation, tubulin was purified by DEAE-Sepharose column chromatography using FPLC (Pharmacia, Uppsala, Sweden). Pure tubulin was obtained by eluting the column with 0.7 M NaCl. MAP2 was purified from the crude microtubule proteins by boiling in the presence of 0.8 M NaCl and 50 mM β-mercaptoethanol followed by the separation using Superdex 200 gel filtration (Pharmacia, Uppsala, Sweden).

In the usual preparation of microtubule proteins, GTP was used for tubulin polymerization. When the phosphorylation of MAP2 by endogenous kinases was examined, ATP was used instead of GTP during the first cycle of the polymerization process. GTP required for tubulin polymerization was produced from GDP and ATP by nucleotide diphosphate kinase that is associated with microtubules (*37*). The catalytic subunit of cAMP-dependent protein kinase (PKA) was purified from bovine cardiac muscle by the method of Beavo et al. (*38*). Cyclin B/cdc2 kinase was purified from starfish oocytes at the first meiotic M phase by $p13^{suc1}$ affinity chromatography (*39*, *40*). The catalytic activities of PKA and cdc2 kinase were determined by phosphorylation of histone H1 (*14*). All protein preparations were frozen in liquid N_2 and stored at −80 °C until they were used.

Phosphorylation of MAP2. MAP2 was phosphorylated using the catalytic subunit of PKA (specific activity = 0.5 nmol of Pi mg^{-1} min^{-1}) or cyclin B/cdc2 kinase (specific activity = 0.5 nmol of Pi mg^{-1} min^{-1}) in 20 mM MOPS (pH 7.5), 5 mM $MgCl_2$, and 0.1 mM ATP for 90−120 min at 30 °C. Throughout the experiments, we used active forms of both kinases: the catalytic subunit of PKA for PKA-dependent phosphorylation and cyclin B/cdc2 kinase for cdc2 kinase-dependent phosphorylation. The reactions were stopped by boiling in the presence of 0.5 M NaCl for 5 min. Denatured kinases were removed by ultracentrifugation at 100000*g* for 30 min. The phosphorylated MAP2 obtained in the supernatant was dialyzed against PM buffer [0.1 M PIPES (pH 6.9), 0.5 mM $MgSO_4$, and 1 mM EGTA] to decrease the salt concentration. For unphosphorylated MAP2, similar procedures of boiling in NaCl and dialysis were also carried out. To determine the stoichiometry of phosphorylation, 0.625 μM MAP2 was incubated in the above solution containing 0.1 MBq of [γ-^{32}P]ATP, and the reaction was carried out for 10−150 min. To determine

whether any endogenous kinases are contaminated in the MAP2 preparation, MAP2 was incubated under the same reaction conditions but without exogenous kinases. Reactions were stopped by boiling after the addition of SDS−PAGE sample buffer, and proteins were separated on 8% polyacrylamide gels and stained with Coomassie Brilliant Blue R. After the gel was destained, bands of MAP2 were cut out and incorporated ^{32}P was estimated by Cerenkov radiation. The stoichiometry of phosphorylation was calculated assuming that the molecular mass of MAP2 is 200 kDa according to the amino acid sequence data of mouse MAP2 (*41*).

Examination of Phosphorylated Regions of MAP2. Phosphorylated sites of MAP2 were determined by limited proteolytic digestion. MAP2 (0.625 μM) was phosphorylated by PKA or by cdc2 kinase in the presence of 0.1 MBq of [γ-^{32}P]ATP for 90 min and then digested by 0.1 μg/mL trypsin for 2 min (*42*). The digestion reaction was stopped by the addition of 1 μg/mL soybean trypsin inhibitor. The digested MAP2 samples were mixed with 5.2 μM microtubules which had been polymerized in the presence of 20 μM paclitaxel and incubated at 37 °C for 20 min. Microtubules were then spun down at 100000*g* for 30 min at 37 °C using a TL-100 ultracentrifuge (Beckman, Palo Alto, CA). Aliquots of the supernatants and pellets were electrophoresed on 10% SDS−PAGE gels followed by autoradiography on Kodak XO-MAT X-ray film. The ratio of ^{32}P in the pellets and in the supernatants was also estimated by densitometry of the film using a laser densitometer (ULTROSCAN 2022, LKB, Uppsala, Sweden).

Binding of MAP2 on Microtubules. The amount of MAP2 bound to microtubules was determined by a cosedimentation experiment as follows. MAP2 (0.25 μM), which had been phosphorylated by PKA or by cdc2 kinase, and 5 μM tubulin in PM buffer containing 0.5 mM GTP were incubated at 37 °C in the presence of 20 μM paclitaxel for 20 min. After NaCl was added at various concentrations, samples were further incubated for 10 min. Microtubules were then centrifuged at 100000*g* for 30 min at 37 °C using a TL-100 ultracentrifuge, and aliquots of the supernatants and pellets were examined with SDS−PAGE. The ratio of bound MAP2/total MAP2 was estimated by densitometric scanning (ACI-Japan, Tokyo, Japan).

Observation of Microtubule Dynamics. The dynamic behavior of microtubules was observed using dark-field microscopy and analyzed with a computer-based analysis system as described previously (*11*). Microtubules were polymerized in PM buffer containing 1 mM GTP. Oxygen radicals generated by the strong illumination used in dark-field microscopy readily break down the microtubules, so 2.16 mg/mL glucose oxidase, 0.36 mg/mL catalase, and 0.25 M glucose were added to remove free oxygen from the solution (*43*). Thirty microliters of a solution of tubulin (32 μM) was incubated at 37 °C for 5 min to allow the spontaneous formation of microtubules. An equal volume of MAP2 (0.5 μM) with various phosphorylation states was then added to the microtubule solution, after which it was transferred onto a glass slide. Microtubules were observed at room temperature which was kept between 24 and 26 °C and were observed with a microscope (BHF, Olympus, Tokyo, Japan) equipped with an oil-immersion dark-field condenser for high-magnification objectives (Olympus DC, numerical aperture of 1.2−1.33) and a 100× Planapo objective lens with an iris (Zeiss, Oberkochen, Germany). The illumination source was a 200 W high-pressure mercury lamp (Osram, GmbH, Berlin, Germany). Images of microtubules were recorded onto a $^1/_2$ in. SVHS videotape using an SIT camera (C-2400-08, Hamamatsu Photonics, Hammatsu, Japan) and a Panasonic model AG 3750 videocassette recorder.

Changes in microtubule length were measured from the video images as previously described (*4*) with some minor modifications. We used a computer-based analysis system to follow the change in length in real time. An arrow-shaped cursor, generated on a personal computer (PC-9801 DA41, NEC, Tokyo, Japan), was electronically overlaid on a video monitor with the aid of a superimposer (PSI400, I. C. Corp., Tokyo, Japan). The change in length at each end of a given microtubule was followed by determining the distance between each end and an arbitrary fixed point on the microtubule.

The microtubule-nucleating activity of MAP2 was examined as follows. A solution of 30 μM tubulin and 0.3 μM MAP2 was mixed at 0 °C. Five microliters of the mixture was transferred onto a dust free glass slide, mounted with a dust free 22 mm × 22 mm cover slip, and immediately examined using dark-field microscopy. Microtubule polymerization was automatically initiated by increasing the temperature from 0 °C to room temperature (27 °C), and growth of microtubules was recorded as was done for microtubule dynamics. To quantitate the amount of microtubules polymerized, recorded images were digitized. The whole area of each image was 46 μm × 35 μm and the depth of the specimen 10 μm, so the amount of microtubules in 16 pL of solution was always measured. The white area of each image was calculated with a digital image analyzer (IBAS, Zeiss, Oberkochen, Germany) for the amount of polymers at any given time after transfer of the samples. Images were enhanced before photographs were taken with a color image recorder (CIR-300, Nippon Avionics Co., Tokyo, Japan).

Miscellaneous. The purities of the protein preparations were determined by SDS−PAGE (*44*), with Coomassie Brilliant Blue R or silver staining (Silver Stain Kit, Wako, Osaka, Japan). All protein concentrations were estimated with the bicinchoninic acid protein assay reagent (Pierce Chemical Co., Rockford, IL) using BSA as a standard. Protein concentrations were also estimated by the densitometric measurements of SDS−PAGE gels stained with Coomassie Brilliant Blue R, known amounts of BSA being electrophoresed in the different lanes of the same gels as standards. The difference in MAP2 concentrations measured by these two procedures was less than ±0.1 μM in the stock solutions whose concentrations ranged between 2.5 and 5 μM, a negligible difference in estimating the molar ratio of phosphorylation.

The molar ratio of phosphoryl groups which originally bound to MAP2 per MAP2 was determined by the method of Hisanaga and Hirokawa (*45*), as follows. MAP2 was reduced to ash over a strong flame after the addition of 10% $Mg(NO_3)_2 \cdot 6H_2O$ in ethanol and solubilized in 1.2 N HCl. P_i reagent [a mixture of 1 volume of 10% (w/v) ammonium molybdate and 3 volumes of 0.2% malachite green] was then added to this solution, and after 5 min, the amount of P_i was estimated by measuring the absorbance at 660 nm using a KH_2PO_4 solution as a standard.

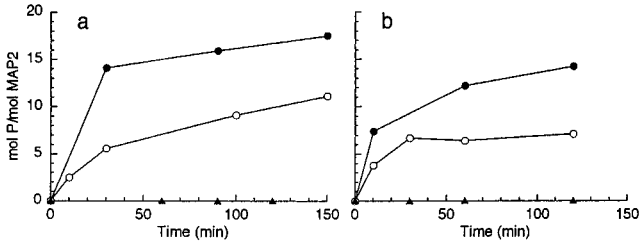

FIGURE 1: Phosphorylation of MAP2. ATP-MAP2 (a) and GTP-MAP2 (b) were phosphorylated by PKA (closed circles) or cdc2 kinase (open circles) as described in the text. When ATP-MAP2 or GTP-MAP2 was incubated in the absence of exogenous kinase (PKA or cdc2 kinase), no phosphorylation occurred (closed triangles at the baseline).

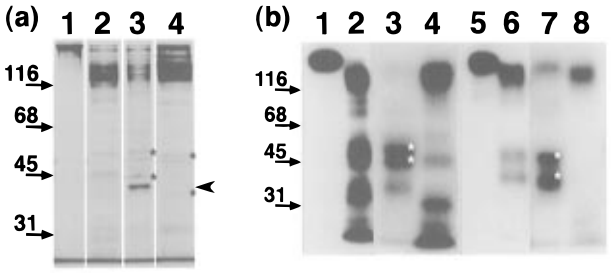

FIGURE 2: Examination of MAP2 phosphorylation sites by partial trypsin digestion. MAP2 was phosphorylated by PKA or cdc2 kinase in the presence of [γ-^{32}P]ATP for 90 min, and the samples were then digested by 0.1 μg/mL TPCK-treated trypsin for 2 min. (a) Comparison of the tryptic digestion patterns of MAP2 in various phosphorylation states: lane 1, untreated native MAP2; lane 2, digested native MAP2; lane 3, digested PKA-phosphorylated MAP2; and lane 4, digested cdc2 kinase-phosphorylated MAP2. The gel was silver-stained to visualize minor bands in digested samples. The major band in lane 3 (indicated by an arrowhead) is the catalytic subunit of PKA. Trace bands indicated by asterisks in lanes 3 and 4 correspond to the bands cosedimented with microtubules in lanes 3 and 7 in panel b (also indicated by asterisks). (b) Cosedimentation of MAP2 fragments with microtubules. Phosphorylated MAP2 and its fragments were visualized by autoradiography as described in the text. Lanes 1 and lane 5 show PKA-phosphorylated MAP2 and cdc2 kinase-phosphorylated MAP2 before digestion. The digested samples (lane 2 for PKA-phosphorylated MAP2 and lane 6 for cdc2 kinase-phosphorylated MAP2) were mixed with microtubules in the presence of paclitaxel and subjected to ultracentrifugation. Fragments of MAP2 bound to microtubules were collected in the pellet (lane 3 for PKA-phosphorylated MAP2 and lane 7 for cdc2 kinase-phosphorylated MAP2), while unbound fragments remained in the supernatant (lane 4 for PKA-phosphorylated MAP2 and lane 8 for cdc2 kinase-phosphorylated MAP2). Arrows in panels a and b indicate positions of standard molecular mass markers.

RESULTS

The Number of Phosphoryl Groups on MAP2 Depends upon the Type of Nucleotide Used in the Microtubule Preparation. To examine the role of the phosphoryl groups that bind to native MAP2, MAP2 with defined phosphorylation states which reflect *in vivo* phosphorylation must be used. The first step of microtubule preparation from crude brain homogenates is the isolation of polymerized microtubules by ultracentrifugation. GTP is usually used as the nucleotide to polymerize microtubules in this step. When MAP2 was purified from microtubules prepared in this manner, 9.9 $\pm$ 2.7 mol (n = 3) of phosphoryl groups was associated per mole of MAP2. However, when ATP was used in place of GTP, the number of phosphoryl groups associated per mole of purified MAP2 increased to 29.2 $\pm$ 0.8 mol (n = 2) since ATP could serve as a phosphate donor for any contaminating kinase(s). To distinguish them, we refer to the former as GTP-MAP2 and to the latter as ATP-MAP2. We also refer to these MAP2 molecules as "native MAP2" because they were not treated with any exogenous enzymes.

Phosphorylation of MAP2 by PKA and cdc2 Kinase. We chose PKA and cdc2 kinase for phosphorylation of MAP2 due to (i) PKA's association with MAP2 and (ii) the similar substrate specificity of cdc2 kinase with respect to brain cdk5 kinase. We examined the stoichiometry of phosphorylation of ATP-MAP2 and GTP-MAP2 to determine whether the basal level of phosphorylation affects the further phosphorylation by PKA or cdc2 kinase. As shown in Figure 1a, PKA incorporated 17 phosphoryl groups into ATP-MAP2, which already possessed 29 phosphoryl groups while cdc2 kinase incorporated 10 additional phosphoryl groups into ATP-MAP2 within 120 min. In the case of GTP-MAP2, which already possessed 10 phosphoryl groups, PKA incorporated 15 additional phosphoryl groups and cdc2 kinase added 7 more phosphoryl groups within 120 min (Figure 1b). The absence of any endogenous kinases in the purified MAP2 preparations was confirmed by incubating the MAP2s in [γ-^{32}P]ATP without exogenous kinases (Figure 1a). To exclude the possibility of phosphate exchange on MAP2, 2 mM nonlabeled ATP was added into the reaction mixture after 120 min of phosphorylation and the mixture was further incubated for 120 min. If phosphate exchange had occurred, the incorporated radioactive phosphate would decrease during the chase with nonlabeled ATP. However, no decrease in the radioactivity associated with MAP2 was detected, even after 120 min of additional incubation (data not shown). These results indicated that incorporated phosphoryl groups reflect the actual phosphorylation rather than exchange, and that the differences in the basal level of phosphorylation do not affect additional phosphate incorporation by either PKA or cdc2 kinase.

We determined the rough distribution of phosphorylation sites on MAP2 following phosphorylation by PKA or cdc2 kinase using partial trypsin digestion. The tryptic digestion patterns of MAP2 were slightly different depending on the phosphorylation states, as shown in Figure 2a. Thirty-eight percent of the phosphoryl groups of PKA phosphorylation located in the MAP2 fragments cosedimented with microtubules (Figure 2b, lanes 3 and 4). On the other hand, 60% of phosphoryl groups were associated with microtubule-binding fragments of cdc2 kinase-phosphorylated MAP2 (Figure 2b, lanes 7 and 8).

Phosphorylation Decreases Binding of MAP2 to Microtubules. To understand the effects of MAP2 phosphorylation on the regulation of microtubule dynamics, we compared (i) the microtubule-binding activity, (ii) the dynamics of individual microtubules, and (iii) the microtubule-nucleating activity between the above MAP2 preparations in different phosphorylation states.

Salt dependency of MAP2−microtubule binding is a good criterion for the MAP2-binding activity to microtubules (*46*). In the absence of NaCl, all native MAP2 cosedimented with paclitaxel-stabilized microtubules and unbound MAP2 could not be detected in the supernatant. All MAP2 phosphorylated by PKA or cdc2 kinase, as well as native MAP2, bound to microtubules as native MAP2 in the absence of NaCl, a value assigned as 100% which was independent of the states

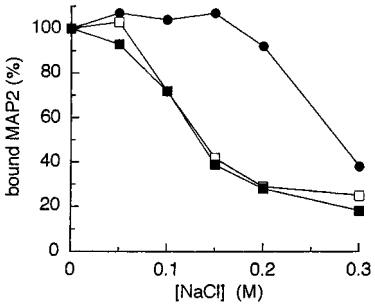

FIGURE 3: Salt desorption of native MAP2, PKA-phosphorylated MAP2, or cdc2 kinase-phosphorylated MAP2 from microtubules. Native MAP2 (closed circles), PKA-phosphorylated MAP2 (open squares), and cdc2 kinase-phosphorylated MAP2 (closed squares) were incubated with microtubules at 37 °C in the presence of 20 μM paclitaxel for 20 min. After NaCl was added at various concentrations, the samples were further incubated for 10 min. Then microtubules were sedimented at 100000*g* for 30 min at 37 °C, and the supernatants and pellets were examined by SDS−PAGE. For normalization, the amount of native MAP2 bound to microtubules in the absence of NaCl was assigned as 100%. Without NaCl, no unbound MAP2 was detected in the supernatant.

of phosphorylation (Figure 3). Native MAP2 could not be desorbed from microtubules at lower salt concentrations of up to 0.15 M, and was gradually released only at higher salt concentrations. In contrast to native MAP2, phosphorylated MAP2 was released from microtubules more readily at significantly lower salt concentrations. However, the salt sensitivity of the MAP2-binding activity to microtubules was similar for PKA-phosphorylated MAP2 and cdc2 kinase-phosphorylated MAP2 (compare filled and open squares in Figure 3).

The Activity of MAP2 That Modulates Microtubule Dynamics Depends on Its Phosphorylation State. The effects of MAP2 phosphorylation with various kinases have been previously studied using turbidimetry of microtubule polymers, under which conditions clear differences among various kinases could not be detected. By turbidimetric criteria, all kinases examined similarly inhibited the activity of MAP2 on microtubule polymerization (*20*−*22*, *25*, *28*, *47*). The effects of MAP2 phosphorylation on individual microtubule dynamics thus remained to be examined. We addressed this question by comparing the behavior of individual microtubules in the presence of MAP2 with different phosphorylation states using dark-field microscopy. MAP2 at various levels of phosphorylation was added to the microtubules which had spontaneously polymerized from 32 μM pure tubulin at 37 °C. The final tubulin concentration was 16 μM, and the MAP2 concentration was 0.25 μM. These microtubules were quite labile in the absence of MAPs (Figure 4a), probably due to the decrease in temperature (37 to 24−26 °C) and the dilution, as previously reported (*11*). The frequency of rescue (i.e., the phase transition from depolymerization to polymerization) at the plus end of these microtubules was especially low, as previously reported by Walker et al. (*5*).

The addition of 0.25 μM native MAP2 did not increase the number of microtubules visible in the microscopic field, and no short microtubules were observed, indicating that nucleation of microtubules did not occur. The added MAP2 probably bound to preformed microtubules preferentially. In the presence of native MAP2, microtubules easily underwent rescue, as shown in Figure 4b, although the frequency of catastrophes decreased slightly. As a result, the half-life of

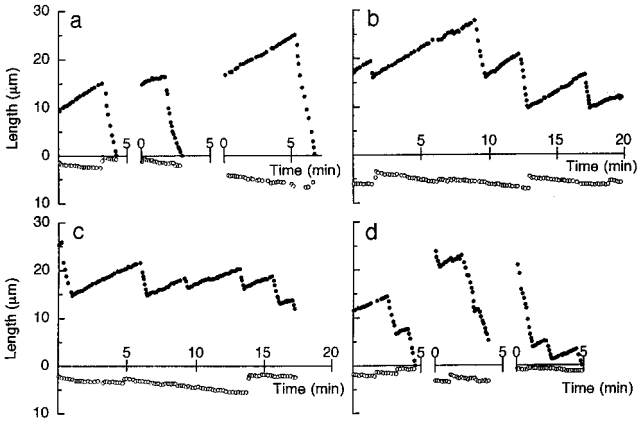

FIGURE 4: Changes in length at both the plus and minus ends of individual microtubules in the absence of MAP2 (a) or in the presence of native MAP2 (b), PKA-phosphorylated MAP2 (c), or cdc2 kinase-phosphorylated MAP2 (d). The concentrations of tubulin and MAP2 were 16 and 0.25 μM, respectively. The filled and open circles show the plus and minus ends of the microtubule, respectively. To emphasize that all microtubules depolymerized within 5 min, length changes of three different microtubules are shown in panels a and d. For clarity, length change profiles observed simultaneously were shifted horizontally.

individual microtubules was longer than that in the absence of MAP2. Thus, native MAP2 protected microtubules against the depolymerization induced by both lowering temperature and dilution. These protective effects were observed similarly in the presence of ATP-MAP2 or GTP-MAP2, and the dynamic behavior of microtubules at the plus end was more strongly modulated by MAPs than that at the minus end (*11*). Indeed, the stabilizing effect of MAP2 was due to an increase in the frequency of rescues at the plus end (Table 1), and no obvious change could be detected at the minus end (data not shown). The effects of phosphorylated MAP2 on the plus end dynamics were therefore analyzed in greater detail. Since the velocities of polymerization and depolymerization did not change significantly, the polymerization length prior to a catastrophe increased slightly and the depolymerization length prior to a rescue decreased significantly. The microtubule-stabilizing activity of MAP2 was similar to those of GTP-MAP2 and ATP-MAP2 in terms of the parameters of dynamic instability.

The profile of the typical change in microtubule length in the presence of MAP2 phosphorylated by PKA was similar to that in the presence of native ATP-MAP2 (Figure 4c). The four parameters of dynamic instability were almost equal to those in native MAP2 (Table 1), suggesting that the stabilizing effects of MAP2 were not changed by the phosphorylation with PKA. Comparable results were obtained with either ATP-MAP2 or GTP-MAP2, indicating that the basal level of MAP2 phosphorylation had no influence upon the PKA-dependent phosphorylation.

In contrast, phosphorylation of ATP-MAP2 by cdc2 kinase significantly decreased its microtubule-stabilizing activity. Microtubules disappeared completely within 5 min, even in the presence of MAP2 phosphorylated by cdc2 kinase, as occurred in the absence of MAP2 (Figure 4d), although rescues were slightly more frequent than in the absence of MAP2. The decreased stability of microtubules was due to a lowering of the frequency of rescues (Table 1). The GTP-MAP2 phosphorylated by cdc2 kinase was also unable to stabilize microtubules.

Table 1: Effects of Various States of MAP2 Phosphorylations on Microtubule Dynamics at Plus Ends[a]

	growth rate (μm/min)	shortening rate (μm/min)	catastrophe frequency (s^{-1})	rescue frequency (s^{-1})	growth length (μm)[b]	shortening length (μm)[b]
MAP free ($n = 18$)	1.26 ± 0.39	9.83 ± 2.91	0.006	0.005	3.55	30.08
ATP-MAP2						
unphosphorylated ($n = 8$)	1.43 ± 0.32	12.26 ± 4.46	0.006	0.029	4.27	7.54
phosphorylated by PKA ($n = 8$)	1.35 ± 0.45	11.11 ± 4.96	0.008	0.032	2.63	6.36
phosphorylated by cdc2 ($n = 16$)	1.23 ± 0.40	13.54 ± 5.57	0.010	0.015	2.22	16.46
GTP-MAP2						
unphosphorylated ($n = 10$)	1.25 ± 0.39	11.09 ± 4.66	0.008	0.035	2.81	5.37
phosphorylated by PKA ($n = 11$)	1.24 ± 0.44	10.16 ± 4.76	0.008	0.037	2.42	5.11
phosphorylated by cdc2 ($n = 14$)	1.29 ± 0.47	11.91 ± 5.62	0.012	0.016	1.75	13.12

[a] The tubulin concentration was 16 μM and the MAP2 concentration 0.25 μM for all experiments. [b] The growth or shortening length was calculated by dividing the total number of transitions by the summed length of either phase.

Both PKA and cdc2 Kinase Decreased the Microtubule-Nucleating Activity of MAP2. Although PKA did not change the microtubule-stabilizing ability of MAP2, cdc2 kinase did. However, earlier turbidimetric investigations had shown that phosphorylation of MAP2 by PKA inhibited MAP2-stimulated microtubule polymerization (*20*, *47*). In those previous studies, pure tubulin and phosphorylated MAP2 were mixed before initiating the polymerization reaction, and the effect of phosphorylation of MAP2 on the initial step of polymerization, i.e., the nucleation, remained to be examined. To test this possibility, we characterized the effect of MAP2 phosphorylation on the spontaneous polymerization of microtubules. Although microtubules self-assembled without MAPs at 37 °C, as described above, no microtubules were formed at room temperature (24−27 °C), and lower temperatures were not sufficient to allow the self-assembly of microtubules at these tubulin concentrations (30 μM). However, microtubules did self-assemble in the presence of native MAP2 even at room temperature; microtubules appeared within 6 min in such numbers that individual microtubules could not be distinguished (top row of Figure 5, filled circles in Figure 6).

In the presence of MAP2 phosphorylated by PKA, only a small number of microtubules was formed within 6 min, quite in contrast to those formed with native MAP2. However, once microtubules were formed, their length tended to increase during the observation period (middle row of Figure 5). This contributed slightly to the increase observed in the total amount of polymer (compare filled circles and open triangles in Figure 6). The effect of the phosphorylation by cdc2 kinase on the nucleation of microtubules was more dramatic. No microtubule appeared even 11 min after the polymerization reaction was initiated (bottom row of Figure 5, filled triangles in Figure 6). These results show that (i) PKA-dependent phosphorylation of MAP2 suppresses the microtubule-nucleating activity of MAP2 without inhibiting its microtubule-stabilizing activity and (ii) cdc2 kinase-dependent phosphorylation of MAP2 completely inhibits both activities.

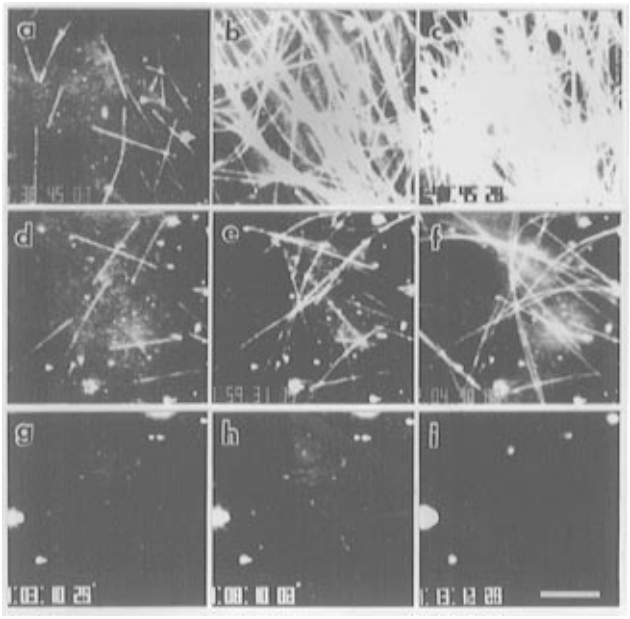

FIGURE 5: Spontaneous nucleation of microtubules in native MAP2 (a−c), PKA-phosphorylated MAP2 (d−f), and cdc2 kinase-phosphorylated MAP2 (g−i). A solution of 30 μM tubulin and 0.3 μM MAP2 was mixed at 0 °C and transferred onto a glass slide. Microtubule polymerization was initiated by increasing the temperature from 0 to 27 °C, and specimens were examined immediately using dark-field microscopy so that the first micrographs (a, d, and g) were taken 1 min after the initiation. The second micrographs (b, e, and h) were taken at 6 min, and the third micrographs (c, f, and i) were taken at 11 min. Bar = 10 μm.

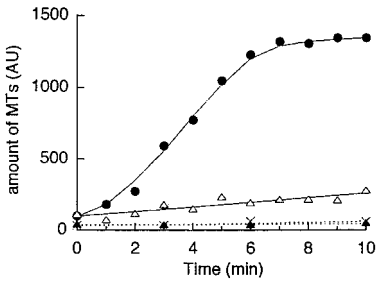

FIGURE 6: Changes in the amount of microtubules determined from video images. Dark-field images at given times were digitized, and the white area of all images was measured with a digital image analyzer for the amount of polymers: native MAP2 (closed circles), PKA-phosphorylated MAP2 (open triangles), cdc2 kinase-phosphorylated MAP2 (closed triangles), and no MAP2 (×).

DISCUSSION

Phosphorylation States of Native MAP2. We demonstrate in this study that the number of phosphoryl groups on native MAP2 depends on the type of nucleotides contained in the tubulin-polymerizing buffer. As described above, MAP2 prepared in ATP-containing buffer (ATP-MAP2) possesses 29 mol of phosphoryl groups, while that prepared in GTP-containing buffer (GTP-MAP2) has only 10 mol, as reported previously (*20*). The difference in the number of phosphoryl groups must be due to phosphorylation or dephosphorylation

during the first step of microtubule preparation. In the absence of ATP, phosphoryl groups on MAP2 in the homogenate are partly removed by the phosphatase(s). On the other hand, in the presence of ATP, kinase(s) could catalyze a counter-reaction so that the number of phosphoryl groups per MAP2 molecule increases. However, we cannot predict differences in phosphorylation sites between ATP-MAP2 and GTP-MAP2 that are already phosphorylated. Despite the difference in the phosphorylation level, both ATP-MAP2 and GTP-MAP2 are similar to each other as the substrates for either PKA or cdc2 kinase. These results indicate that phosphorylation states in native MAP2 have no influence on subsequent phosphorylation by either PKA or cdc2 kinase.

PKA phosphorylates approximately 15 mol per mole of MAP2, a value comparable to that obtained by Murthy and Flavin (*20*). In contrast, cdc2 kinase phosphorylates up to 10 mol per mole of MAP2, a value higher than that obtained by Faruki et al. (*26*), where cdc2 kinase phosphorylated about 4 mol per mole of MAP2. For the cdc2-dependent phosphorylation, Faruki et al. used *Xenopus* egg extracts, which contain various factors. Because we used purified cdc2 kinase, the difference in the phosphate incorporation is due to the conditions and enzyme preparations.

PKA Primarily Phosphorylates the Projection Region of MAP2 while cdc2 Kinase Phosphorylates the Microtubule-Binding Region. Partial trypsin digestion experiments suggested that PKA phosphorylates approximately two-thirds of the total phosphoryl groups into the projection domain of MAP2, which may not be involved in microtubule binding. In contrast, the microtubule-binding domain of MAP2 is phosphorylated more efficiently by cdc2 kinase. The consensus sequences for phosphorylation differ between these two kinases. In the primary sequence of mouse MAP2 (*41*), consensus sequences for PKA [RXX(S/T), RRX(S/T), KXX-(S/T), or KKX(S/T)] (*48*) are distributed primarily in the projection part. The consensus sequence for cdc2 kinase is (S/T)PX(K/R), but (S/T)P sequences are shown to be phosphorylated in various substrates (*49*, *50*). In fact, several proline-directed kinases, including cdc2 kinase, have been reported to phosphorylate the second and third Thr residues of $_{1616}$RTPGTPGTPSY$_{1626}$ in the proline rich region of MAP2 (*51*), the region at the N-terminal side of the microtubule-binding region. Sequences of (S/T)PX(K/R) or (S/T)P are enriched in the C-terminal part of MAP2, which includes the microtubule-binding region and the proline rich region. It is likely that the different effects of MAP2 phosphorylation on microtubule dynamics are due to the differences in phosphorylation sites which in turn depend on the kinases.

Phosphorylation of MAP2 Modifies Its Microtubule-Binding, -Stabilizing, and -Nucleating Activities. In this study, we compared the various effects of MAP2 phosphorylation by PKA and by cdc2 kinase and characterized its (i) microtubule-binding activity, (ii) dynamics of individual microtubules, and (iii) microtubule-nucleating activity. Among them, the microtubule-nucleating activity is the most sensitive to the phosphorylation states of MAP2. Phosphorylation by PKA suppresses the microtubule-nucleating activity of MAP2 without altering its microtubule-stabilizing activity, while phosphorylation by cdc2 kinase suppresses both activities. It is likely that MAP2 partially loses its activities upon phosphorylation by PKA, whereas MAP2 completely loses them upon the phosphorylation by cdc2 kinase.

Phosphorylation does not eliminate the microtubule-binding activity of MAP2 in the absence of NaCl, but increased concentrations of NaCl distinguish it from that of unphosphorylated MAP2. However, we did not detect differences in salt dependency of MAP2 release from microtubules between PKA-catalyzed and cdc2 kinase-catalyzed phosphorylation. This is in contrast to the effects on microtubule dynamics which distinguished the PKA-phosphorylated MAP2 from the cdc2-phosphorylated MAP2. This may be due to the decreased sensitivity of binding experiments to phosphorylation. Otherwise, the decrease in the rescue-dependent microtubule-stabilizing activity of MAP2 seems not to be directly related to the increase in the salt sensitivity of MAP2 binding to stable microtubules.

MAP2 (0.25 μM) bound completely to 5 μM microtubules, independent of the phosphorylation states, in the absence of NaCl (Figure 3). Microtubule dynamics were observed under conditions virtually identical to those of the binding experiments. This tubulin concentration is comparable to the estimated polymer-state tubulin concentration ($\sim$6 μM) employed for dark-field microscopic observation (*11*), and the number of microtubules at the beginning of microscopic observation was similar whenever any of the phosphorylation states of MAP2 was added. These data indicate that microtubules should bind the same amount of MAP2 initially, regardless of the phosphorylation states. Nevertheless, PKA-phosphorylated MAP2, as well as native MAP2, increased the frequency of rescue, whereas cdc2-phosphorylated MAP2 did not. This means that microtubule-stabilizing activity is not simply determined by the total amount of MAP2 on microtubules but rather that the mode of its binding to microtubules can be important. Phosphorylation may change the mode of binding of MAP2 onto microtubules. MAP2 cooperatively binds to microtubules in clusters (*11*, *52*), and this cooperative binding may cause the strong rescue activity against depolymerization. The cooperative binding of MAP2 could be altered differently upon phosphorylation by PKA or cdc2 kinase.

PKA-Dependent Phosphorylation of MAP2. We demonstrated in this study that PKA-dependent phosphorylation of MAP2 suppresses its microtubule-nucleating activity without inhibiting its microtubule-stabilizing activity, although a small number of microtubules could be nucleated (Figure 6). Using an experimental system similar to ours, Murthy and Flavin (*20*) found that PKA-dependent phosphorylation of MAP2 reduced the rate of turbidity increase without changing the critical concentration for polymerization. Considering that the initial rate of turbidity increase is determined by the number of nuclei, their results suggest that PKA-dependent phosphorylation suppresses the nucleation step only, which is consistent with our conclusion. Using microscopic observations, we were able to follow the events occurring in individual microtubules and could determine the effects of PKA phosphorylation on MAP2 activity more precisely. Phosphorylation of MAP2 by PKA is not critical for reducing the rescue frequency but is critical for suppressing a more sensitive step, the nucleation, as reported by Jameson and Caplow (*47*) in phosphorylated crude MAPs in the presence of cAMP. Although Raffaelli et al. (*52*) showed that autophosphorylation of MAPs in the presence of cAMP destabilized microtubules, the difference in their results with respect to those reported by Jameson

and Caplow (*47*) may be due to kinases in the crude MAP fraction.

cdc2 Kinase-Dependent Phosphorylation of MAP2. We further show in this study that cdc2 kinase-dependent phosphorylation of MAP2 reduces both its microtubule-stabilizing and its microtubule-nucleating activities. Faruki et al. have reported that phosphorylation of MAP2 by cdc2 kinase in *Xenopus* egg extracts does not significantly alter its ability to stabilize microtubules (*26*). Such a difference is probably due to the amounts of MAP2 used in these two studies. We added 0.25 μM MAP2 to 16 μM tubulin, which was within a cooperative binding range (*52*). On the other hand, Faruki et al. (*26*) added MAP2 to tubulin at a molar ratio of about 1/10, which is above the saturation binding range. A greater amount of MAP2 might enhance the stability of microtubules even if the affinity of each MAP2 is decreased by phosphorylation. Indeed, when the amount of cdc2 kinase-phosphorylated MAP2 is increased, microtubules become stable as was observed with unphosphorylated MAP2 (data not shown). Alternatively, the difference may simply be due to the amount of phosphate incorporation.

Physiological Role of Phosphorylation of MAP2. A greater amount of phosphate incorporation by PKA did not alter the microtubule-stabilizing activity of MAP2, but a smaller amount of phosphate by cdc2 kinase did. The extent of phosphorylation on MAP2 is not the determinant that modifies MAP2 activity. Brugg and Matus (*53*) showed that binding of MAP2 to microtubules depends on the states of its phosphorylation when microinjected into cultured cells that do not express endogenous MAP2. They suggested that the sites of phosphate incorporation on MAP2 are essential to microtubule binding and that the amount is not a critical factor. Our present results are in agreement with theirs. It may be that each phosphorylation site of MAP2 may have a different role for microtubule function and that phosphorylation of each site may be catalyzed by different kinases.

The amount of phosphate added to MAP2 by PKA or cdc2 kinase does not depend on the initial states of phosphorylation, suggesting that the additional 19 mol per mole of phosphorylation in ATP-MAP2 does not involve PKA or cdc2 kinase. One might suspect that phosphorylation by PKA or cdc2 kinase is not physiologically relevant because of their low activities in brain homogenates. However, PKA is active only in the presence of cAMP (*54*), so its activity must be low in our preparations to which no cAMP was added. The level of cAMP is controlled by the stimulation of serotonin in *Aplysia* sensory neuron (*55*) or by NMDA receptor activation in mammalian hippocampus (*56*). It is possible that the PKA-dependent phosphorylation of MAP2 is also related to the neuronal plasticity in mammalian brain. We used cdc2 kinase to investigate the effects of the proline-directed phosphorylation of MAP2 in these experiments. Since cdc2 kinase has been shown to phosphorylate tau at the same sites as cdk5 kinase (*33*), we assume that both kinases have similar substrate specificities in MAP2 and tau. Since the activity of cdk5 kinase is relatively low in adult rat brain (*57*), it may be locally activated among the huge number of neurons. Thus, it is conceivable that the total activity of cdk5 kinase was low in our crude homogenates. Its activity is rather high just before and after birth in rat (*57*), suggesting that the phosphorylation of MAP2 by this kinase is related to brain development. The phosphorylation states of MAP2 in neurons is regulated by the activity of glutamate receptors (*58, 59*). In cultured hippocampal neurons, levels of phosphorylation increase with the dendrite extension (*60*). It is possible that regulation of the MAP2 phosphorylation states plays an important role in neuronal plasticity by regulating microtubule dynamics. In dendrites of neuronal cells, the dynamics and/or organization of microtubules can be regulated by controlling the available amount of MAP2 through phosphorylation by kinases such as PKA or cdk5. Further experiments to test these hypotheses are currently in progress in our laboratory.

ACKNOWLEDGMENT

The authors thank Mr. H. Kitazawa and Ms. S. Koike for their help with the data analysis. The authors are also grateful to Dr. H. Yamamoto for valuable suggestions.

REFERENCES

1. Dustin, P. (1984) *Microtubules*, 2nd ed., Springer-Verlag, Berlin.
2. Hyams, J. S., and Lloyd, C. W. (1994) *Microtubules*, Wiley-Liss, New York.
3. Mitchison, T. J., and Kirschner, M. W. (1984) *Nature 312*, 237−242.
4. Horio, T., and Hotani, H. (1986) *Nature 321*, 605−607.
5. Walker, R. A., O'Brien, E. T., Pryer, N. K., Soboeiro, M. F., Voter, W. A., Erickson, H. P., and Salmon, E. D. (1988) *J. Cell Biol. 107*, 1437−1448.
6. Cassimeris, L., Pryer, N. K., and Salmon, E. D. (1988) *J. Cell Biol. 107*, 2223−2231.
7. Sammak, P. J., and Borisy, G. G. (1988) *Nature 332*, 724−726.
8. Hotani, H., and Horio, T. (1988) *Cell Motil. Cytoskeleton 10*, 229−236.
9. Pryer, N. K., Walker, R. A., Skeen, V. P., Bourns, B. D., Soboeiro, M. F., and Salmon, E. D. (1992) *J. Cell Sci. 103*, 965−976.
10. Kowalski, R. J., and Williams, R. C., Jr. (1993) *J. Biol. Chem. 268*, 9847−9855.
11. Itoh, T. J., and Hotani, H. (1994) *Cell Struct. Funct. 19*, 279−290.
12. Panda, D., Goode, B. L., Feinstein, S. C., and Wilson, L. (1995) *Biochemistry 34*, 11117−11127.
13. Matus, A. (1994) in *Microtubules* (Hyams, J. S., and Lloyd, C. W., Eds.) pp 155−166, Wiley-Liss, New York.
14. Ookata, K., Hisanaga, S., Bulinski, J. C., Murofushi, H., Aizawa, H., Itoh, T. J., Hotani, H., Okumura, E., Tachibana, K., and Kishimoto, T. (1995) *J. Cell Biol. 128*, 849−862.
15. Kishimoto, T. (1994) *Int. J. Dev. Biol. 38*, 185−191.
16. Shiina, N., Moriguchi, T., Ohta, K., Gotoh, Y., and Nishida, E. (1992) *EMBO J. 11*, 3977−3984.
17. Kreis, T., and Vale, R. (1992) *Guidebook to the cytoskeletal and motor proteins*, Oxford University Press, Tokyo.
18. Tsuyama, S., Terayama, Y., and Matsuyama, S. (1987) *J. Biol. Chem. 262*, 10886−10892.
19. Sloboda, R. D., Rudolph, S. A., Rosenbaum, J. L., and Greengard, P. (1975) *Proc. Natl. Acad. Sci. U.S.A. 72*, 177−181.
20. Murthy, A. S. N., and Flavin, M. (1983) *Eur. J. Biochem. 137*, 37−46.
21. Yamamoto, H., Fukunaga, K., Tanaka, E., and Miyamoto, E. (1983) *J. Neurochem. 41*, 1119−1125.
22. Schulman, H. (1984) *J. Cell Biol. 99*, 11−19.
23. Hoshi, M., Akiyama, T., Shinohara, Y., Miyata, Y., Ogawara, H., Nishida, E., and Sakai, H. (1988) *Eur. J. Biochem. 174*, 225−230.
24. Ainsztein, A. M., and Purich, D. L. (1994) *J. Biol. Chem. 269*, 28465−28471.
25. Hoshi, M., Ohta, K., Gotoh, Y., Mori, A., Murofushi, H., Sakai, H., and Nishida, E. (1992) *Eur. J. Biochem. 203*, 43−52.
26. Faruki, S., Dorée, M., and Karsenti, E. (1992) *J. Cell Sci. 101*, 69−78.

27. Illenberger, S., Drewes, G., Trinczek, B., Biernat, J., Meyer, H. E., Olmsted, J. B., Mandelkow, E.-W., and Mandelkow, E. (1996) *J. Biol. Chem. 271*, 10834−10843.
28. Burns, R. G., Islam, K., and Chapman, R. (1984) *Eur. J. Biochem. 141*, 609−615.
29. Theurkauf, W. E., and Vallee, R. B. (1982) *J. Biol. Chem. 257*, 3284−3290.
30. Ishiguro, K., Ihara, Y., Uchida, T., and Imahori, K. (1988) *J. Biochem. 104*, 319−321.
31. Ishiguro, K., Takamatsu, M., Tomizawa, K., Omori, A., Takahashi, M., Arioka, M., Uchida, T., and Imahori, K. (1992) *J. Biol. Chem. 267*, 10891−10901.
32. Kobayashi, S., Ishiguro, K., Omori, A., Takahashi, M., Arioka, M., Imahori, K., and Uchida, T. (1993) *FEBS Lett. 335*, 171−175.
33. Hosoi, T., Uchiyama, M., Okumura, E., Saito, T., Ishiguro, K., Uchida, T., Okuyama, A., Kishimoto, T., and Hisanaga, S. (1995) *J. Biochem. 117*, 741−749.
34. Hisanaga, S., Uchiyama, M., Hosoi, T., Yamada, K., Honma, N., Ishiguro, K., Uchida, T., Dahl, D., Ohsumi, K., and Kishimoto, T. (1995) *Cell Motil. Cytoskeleton 31*, 283−297.
35. Murata, M., Itoh, T. J., Kagiwada, S., Hishida, R., Hotani, H., and Ohnishi, S.-I. (1992) *Biol. Cell 75*, 127−134.
36. Karr, T. L., White, H. D., and Purich, D. L. (1979) *J. Biol. Chem. 254*, 6107−6111.
37. Jakob, M., and Huitorel, P. (1979) *Eur. J. Biochem. 99*, 613−622.
38. Beavo, J. A., Bechtel, P. J., and Krebs, E. G. (1974) *Methods Enzymol. 38*, 299−308.
39. Kusubata, M., Tokui, T., Matsuoka, Y., Okumura, E., Tachibana, K., Hisanaga, S., Kishimoto, T., Yasuda, H., Kamijo, M., Ohba, Y., Tsujimura, K., Yatani, R., and Inagaki, M. (1992) *J. Biol. Chem. 267*, 20937−20942.
40. Okumura, E., Sekiai, T., Hisanaga, S., Tachibana, K., and Kishimoto, T. (1996) *J. Cell. Biol. 132*, 125−135.
41. Lewis, S. A., Wang, D., and Cowen, N. J. (1988) *Science 242*, 936−939.
42. Vallee, R. B., and Borisy, G. G. (1977) *J. Biol. Chem. 252*, 377−382.
43. Harada, Y., Sakurada, K., Aoki, T., Thomas, D. D., and Yanagida T. (1990) *J. Mol. Biol. 216*, 49−68.
44. Laemmli, U. K. (1970) *Nature 227*, 680−685.
45. Hisanaga, S., and Hirokawa, N. (1989) *J. Neurosci. 9*, 959−966.
46. Raffaelli, N., Yamauchi, P. S., and Purich, D. L. (1992) *FEBS Lett. 296*, 21−24.
47. Jameson, L., and Caplow, M. (1981) *Proc. Natl. Acad. Sci. U.S.A. 78*, 3413−3417.
48. Pearson, R. B., and Kemo, B. E. (1991) *Methods Enzymol. 200*, 62−81.
49. Nigg, E. A. (1993) *Trends Cell Biol. 3*, 296−301.
50. Nigg, E. A. (1995) *BioEssays 17*, 471−480.
51. Sánchez, C., Tompa, P., Szücs, K., Friedrich, P., and Avila, J. (1996) *Eur. J. Biochem. 241*, 765−771.
52. Wallis, K. T., Azhar, S., Rho, M. B., Lewis, S. A., Cowen, N. J., and Murphy, D. B. (1993) *J. Biol. Chem. 268*, 15158−15167.
53. Brugg, B., and Matus, A. (1991) *J. Cell Biol. 114*, 735−743.
54. Taylor, S. S., Buechler, J. A., and Yonemoto, W. (1990) *Annu. Rev. Biochem. 59*, 971−1005.
55. Bacskai, B. J., Hochner, B., Mahaut-Smith, M., Adams, S. R., Kaang, B.-K., Kandel, E. R., and Tsien, R. Y. (1993) *Science 260*, 222−226.
56. Chetkovich, D. M., Gray, R., Johnston, D., and Sweatt, J. D. (1991) *Proc. Natl. Acad. Sci. U.S.A. 88*, 6467−6471.
57. Uchida, T., Ishiguro, K., Ohnuma, J., Takamatsu, S., Yonekura, S., and Imahori, K. (1994) *FEBS Lett. 355*, 35−40.
58. Halpain, S., and Greengrad, P. (1990) *Neuron 5*, 237−246.
59. Quinlan, E. M., and Halpain, S. (1996) *Neuron 16*, 357−368.
60. Díez-Guerra, F. J., and Avila, J. (1995) *Eur. J. Biochem. 227*, 68−77.

BI962606Z